

O. I. P. E. E. C.

**Bulletin
Bericht
Bollettino** **81**

SIEGE SOCIAL: c/o Laboratoire Central des Ponts et Chausées
Boul. Lefebvre, F 75732 PARIS,
(official registered address for legal purposes only)

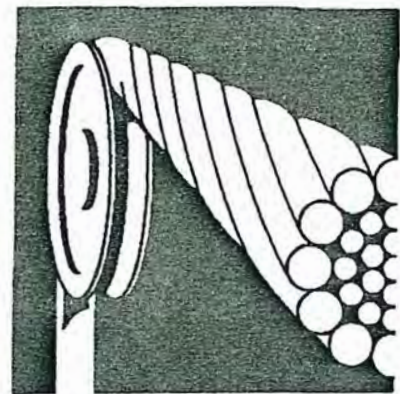
SECRETARIAT: Wire Rope Technology Aachen, Grünenthaler Straße 40a,
D - 52072 Aachen, Germany
(address for correspondence)

COMITE DIRECTEUR

President	D. SAYENGA	USA
Vice-President	G. OPLATKA	ZÜRICH
Membres	R. CIUFFI	FIRENZE
	C.R. CHAPLIN	READING
	J.-P. GOURMELON	NANTES
	J. HANKUS	KATOWICE
	H.M. HUBER	BRUGG
	G.A. KOPANAKIS	ZÜRICH
	I.M.L. RIDGE	READING
	J.-M. TERRIEZ	GRENOBLE
	R. VERREET	AACHEN
	K.-H. WEHKING	STUTTGART
Membres Co-optés	T. BABEU	TIMISOARA
	V. MALINOVSKY	ODESSA
Secrétaire	R. VERREET	AACHEN
Tresorier	G.A. KOPANAKIS	ZÜRICH
Commissaire aux comptes	N. KELLER	ROMANSHORN
Redaction Bulletin	I.M.L. RIDGE	READING

OIPEEC WORKING GROUPS

Working Group 1	Experimental endurance studies Prof. R. Ciuffi - Firenze
Working Group 2	Wire rope publication data base Dipl.-Ing. Roland Verreet - Aachen
Working Group 3	Degradation mechanisms Dipl.-Ing. Georg A. Kopanakis - Zürich
Working Group 4	Wire rope in civil engineering M. Jean Paul Gourmelon - LCPC Nantes
Working Group 5	History of wire rope Mr. Hans Huber - Brugg



O. I. P. E. E. C.

**Bulletin
Bericht
Bollettino**

81

June 2001

ORGANISATION INTERNATIONALE POUR L'ETUDE DE L'ENDURANCE DES CABLES
INTERNATIONAL ORGANISATION FOR THE STUDY OF THE ENDURANCE OF ROPES
INTERNATIONALE ORGANISATION ZUM STUDIUM DER BETREIBSFESTIGKEIT VON SEILEN
ORGANIZZAZIONE INTERNATIONALE PER LO STUDIO DELLA FATICA DELLE FUNI

REDACTION: READING ROPE RESEARCH - READING UNIVERSITY

Department of Engineering - PO Box 225 - Reading RG6 6AY - UK

fax number: (+44) 118 931 3327

OIPEEC Bulletin 81

Copyright © OIPEEC, 2001

Published by : Reading Rope Research

Department of Engineering The University of Reading RG6 6AY, UK

June 2001

Printed by : College of Estate Management

Whiteknights, Reading

ISSN 1018 - 8819

INDEX - INDICE - INHALT

	page
Editorial	4
News from OIPEEC	5
Management Committee Meeting	5
Announcement of OIPEEC Round Table Meeting	6
Abstracts for OIPEEC Round Table Conference Papers	ODN 0703
	7
 Technical Papers:	
Wang, R.C. & McKewan, W.M. <i>A model for the structure of round-strand wire ropes</i>	ODN 0704
	15
Rebel, G., Chaplin, C.R. & Borello, M. <i>Depth limitations in the use of triangular strand ropes for mine hoisting</i>	ODN 0705
	43
Verreet, R. <i>Steel wire ropes with variable lay lengths for mining applications</i>	ODN 0706
	63
Review of Rope Publications	ODN 0707
Instructions for Authors	71
	79

R.C. Wang & W.M. McKewan

Pittsburgh Research Laboratory, NIOSH, Pittsburgh, Pennsylvania

ODN 0704

A model for the structure of round-strand wire ropes

Summary

The behaviour of wire ropes used in mine hoisting is not well understood. In an effort to improve this understanding, the structure of round-strand wire ropes was analysed. This report provides a generalised mathematical model that completely describes the geometry of the wires. It consists of two sets of vector equations and is valid for any round-strand wire rope. One set of equations is used to trace the paths of wires that have the form of a single helix. The other is used for the paths of double helical wires. The specific model for a 33-mm 6x19 Seale, IWRC, right regular lay wire rope was presented as an example. The paths and the geometric properties of the wires which include the path length per lay of strand, the curvature, and the torsion were determined from this model. In future work, the model could be used to conduct stress analysis for the wires in the deformed rope at a given rope strain and also to study the effect of wear and breaking of wires on strength loss for the various round-strand wire ropes used in mine hoisting.

1. Introduction

Wire ropes are used essentially for transmitting tensile forces. The main characteristics which make them so well suited to this function are flexibility and strength. A list of the uses of wire rope is almost endless. In mine hoisting systems, wire rope is used to transport personnel, product and supplies between surface and underground.

The Federal retirement criteria for wire ropes used in mine hoisting specify the allowable reductions of rope diameter and outside wire diameter and the location and number of broken wires and are listed in the Code of Federal Regulations (CFR 1997). However, their effects on strength loss for ropes of different constructions have not been properly considered. This will lead to removing wire ropes from service at different stages where the actual loss of strength is either less or more than what is anticipated. To remedy this deficiency, the knowledge of how the total load is distributed among the wires in different rope constructions needs to be acquired. In general, the load distribution is dependent not only on the cross-sectional area of wires, but also on the specific arrangement of wires in a rope.

The wire stresses in an independent wire rope core (IWRC) were compared by Costello (1990). It was found that, for 17,379 N (3,907 lb) of load applied to the IWRC, the normal stress was 310,264 kPa (45,000 psi) in the central wire of the centre strand and 279,196 kPa (40,494 psi) in the central wire of the outside strand. They were not only significantly different but also considerably higher than 247,591 kPa (35,910 psi), the nominal stress computed by taking the total load and dividing it by the total metallic area. It is, therefore, believed that the load distribution must be considered for different rope constructions in order to prevent catastrophic failure of ropes in service. To do this, an understanding of the wire geometry which affects the

load distribution must be first acquired. Although mathematical models have been used to study wire geometry by many researchers in the past, these models can be used only for single helical wires. Lee (1991) presented two sets of Cartesian co-ordinate equations in matrix form for double helical wires but did not give detailed derivation of the equations. One set of the equations was for regular lay ropes; and the other was for Lang's lay ropes.

In this study, the rope structure was analysed and a generalised mathematical model describing the wire geometry in any rope construction with round strands was developed. The model contains a rotation ratio termed "relative rotation" in this report which characterises the relationship between the wire and the strand helices. In the use of rope with the ends restrained from rotating, this relative rotation remains constant and thus reduces the parameters in the models to the angle of wire rotation only. The model is general enough that any combination of wire and strand lay directions can be handled if the stated sign conventions for the angles of strand and wire rotation and the relative rotation are followed.

2. Description of rope structure

2.1 Structural elements

A wire rope is a structure composed of many individual wires. There are two major structural elements in a typical wire rope. One is the strand which is formed by helically winding wires around a central wire or a strand core. Different shapes of strand may be formed depending on the shape of the core. Only a wire rope made of round strands was analysed in this report. The other major structural element is the core around which the strands are helically wound. The core is made of natural fibres, polypropylene, or steel that will provide proper support for the strands under bending and loading in normal use. The most commonly used cores are fibre core (FC), independent wire rope core (IWRC), and wire strand core (WSC).

Although the strand can be laid in any one of many specific geometric arrangements and composed of any number of wires, the rope also can have any number of strands. The Wire Rope Users Manual (Wire Rope Technical Board, 1993) contains more information on wire rope identification and construction. Most of the rope produced today is pre-formed, meaning that the wires are permanently shaped into the helical form they will assume in the rope. This manufacturing process eliminates the tendency of the wires to unlay, usually hazardously, when they are unrestrained or when the rope is cut.

2.2 Classification of wires

It is assumed in this study that all wires have a circular cross section and remain circular when they are stretched or bent. The centroidal axis which moves through the centre of a wire is selected to represent the path of the wire and used to study its geometric characteristics that are related to wire stress. The centroidal axis of the central wire of a strand also represents the path of the strand.

Based on the structural elements in a wire rope as described above, there is at most one straight wire in a straight rope. It is located in the centre of a WSC or an IWRC rope. All the remaining wires can be classified geometrically into two groups. They are either single helices or double helices. The outer wires in a straight strand used as the WSC have a single helical form because they are helically wound only once

around a straight axis. When a strand is helically wound into a rope, the central wire also has a single helical form. All the other wires have a double helical form because they are wound twice, once around the strand axis and another around the rope axis. However, they remain single helices relative to the central wire of the strand in which they are wound. This relationship is important in the modelling of a double helical wire.

2.3 Structural parameters

The following basic parameters specifying the helical structure are defined and the symbols representing them in the mathematical modelling are shown in parentheses.

Strand helix axis (Z): The axis of the rope around which the strands are helically wound to form a rope, or around which the wires are helically wound to form the centre strand of a rope. The positive direction of the axis is defined to be the direction that the helix advances.

Wire helix axis (W): The centroidal axis of the helical wire around which other wires are helically wound to form a strand. It is also the centroidal axis of a helical strand. The positive direction of the axis is defined to be the direction that the helix advances.

Radius of strand helix (r_s): The perpendicular distance between the centroidal axis of the strand and the strand helix axis.

Radius of wire helix (r_w): The perpendicular distance between the centroidal axis of the wire and the wire helix axis.

Circular helix: The strand helix having a constant helical radius is a circular helix. Similarly, the wire helix having a constant helical radius is also a circular helix.

Angle of strand helix (α_s): The angle of a strand helix at any point along the centroidal axis of the strand is the angle between the tangent vector at that point, heading in the direction that the strand helix advances, and the plane which is perpendicular to the strand helix axis and passes through that point.

Angle of wire helix (α_w): The angle of a wire helix at any point along the centroidal axis of the wire is the angle between the tangent vector at that point, heading in the direction that the wire helix advances, and the plane which is perpendicular to the wire helix axis and passes through that point.

Angle of strand rotation (θ_s): The angle at which the centroidal axis of a helical strand sweeps out in a plane perpendicular to the strand helix axis. The angle is defined to be positive in a right-handed co-ordinate system if a right lay rope is formed and negative if a left lay rope is formed. The angle is expressed in radians unless specified otherwise.

Angle of wire rotation (θ_w): The angle at which the centroidal axis of a helical wire sweeps out in a plane perpendicular to the wire helix axis. The angle is defined to be positive in a right-handed co-ordinate system if a right-hand strand is formed and negative if a left-hand strand is formed. The angle is expressed in radians unless specified otherwise.

Length of strand (L_s): The distance measured parallel to the axis of the rope around which the centroidal axis of a strand or wire makes one complete helical convolution.

Lay length (pitch) of wire (L_w): The distance measured parallel to the wire helix axis around which the centroidal axis of a wire makes one complete helical convolution.

Length of rope (S_r or z): The length measured along the strand helix axis. It represents the distance that a strand helix has advanced on the axis of the rope.

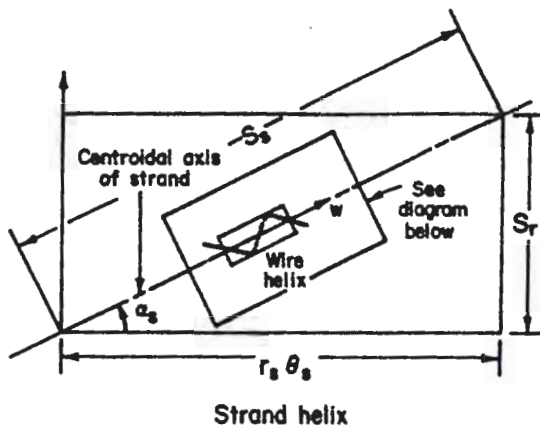
Length of strand (S_s or w): The length measured along the wire helix axis. It represents the distance that a wire helix has advanced on the centroidal axis of the strand.

Length of wire (S_w): The path length measured along the centroidal axis of the wire.

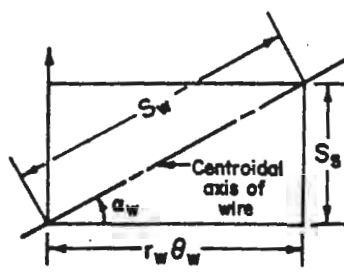
3. Mathematical modelling

3.1 Basic relationships

In circular helices, the centroidal axes of both the wire and the strand may be considered to be lying on right circular cylinders. Because the surface of a cylinder can be developed into a plane, some basic relationships between each of the centroidal axes and the other parameters can be established by using the developed views shown in Figure 1.



Strand helix



Wire helix

Figure 1: Developed views of strand and wire helices

The relationships between the length of rope and the angle of strand rotation and between the length of strand and the angle of strand rotation can be obtained by using the previously defined parameters and from the developed view of the strand helix, which may be expressed as:

$$S_r = r_s \theta_s \tan(\alpha_s) \quad (1)$$

$$S_s = \frac{r_s \theta_s}{\cos(\alpha_s)} \quad (2)$$

The length of rope, S_r in Equation 1 becomes the lay length of the strand, L_s , when $\theta_s = 2\pi$.

Similarly, the relationships between the length of strand and the angle of wire rotation and between the length of wire and the angle of wire rotation also can be obtained by using the developed view of the wire helix and are expressed below.

$$S_s = r_w \theta_w \tan(\alpha_w) \quad (3)$$

$$S_w = \frac{r_w \theta_w}{\cos(\alpha_w)} \quad (4)$$

The length of strand, S_s , in Equation 3 becomes the lay length of wire, L_w , when $\theta_w = 2\pi$.

Since the length of strand obtained from the wire helix must be equal to that obtained from the strand helix for a given length of rope, a new term n is defined to be the ratio of the angle of wire rotation to the angle of strand rotation which can be obtained from Equations 2 and 3.

$$n = \frac{\theta_w}{\theta_s} = \frac{r_s}{r_w \tan(\alpha_w) \cos(\alpha_s)} \quad (5)$$

This ratio is dependent on the angles of both helices when both helical radii are fixed. It is considered to be important in characterising the rope structure, specifically the relationship between the wire and strand helices, and is termed as the "relative rotation" in this report. The relative rotation will be positive for Lang's lay ropes and negative for regular lay ropes.

3.2 Co-ordinate systems

Because several geometric characteristics of helices related to load distribution and wire stresses can be easily evaluated through vector analysis, vector equations describing these helices are used to model the different wires in a rope. To distinguish vectors from scalars, boldface type is used for vectors in the equations. Two three-dimensional, right-handed rectangular Cartesian co-ordinate systems are selected to analyse the strand and wire helices.

One is a global fixed system called, for convenience, the rope co-ordinate system (Figure 2A). The co-ordinates are X, Y, and Z with the origin at the centre of the rope and the Z-axis coinciding with the rope axis. The X-Y plane is perpendicular to the rope axis and is the plane where the angle of strand rotation is measured. The X-axis is arbitrarily selected so that it intersects, in its positive direction, with the centroidal axis of a strand. The X-axis is also used as the reference line from which the angle of strand rotation, θ_s , is measured. The unit vectors directed along the positive directions of X, Y, and Z are \mathbf{i} , \mathbf{j} and \mathbf{k} respectively.

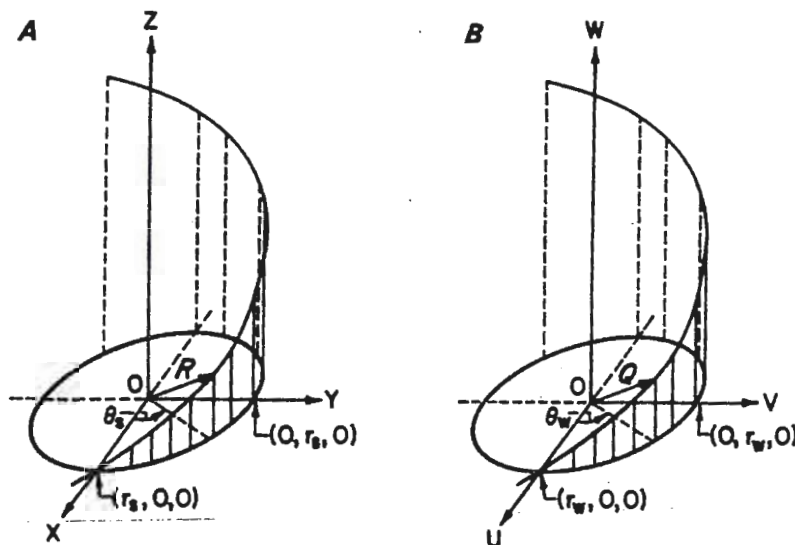


Figure 2: Co-ordinate systems for single helix. A, rope co-ordinate system; B, strand co-ordinate system

The other, a local co-ordinate system, is the strand co-ordinate system (Figure 2B). Its co-ordinates are U, V, and W with the origin on the centroidal axis of a strand. This local co-ordinate system moves along the centroidal axis of the strand. The W-axis is in the direction of the tangent vector to the centroidal axis of the strand. The U-V plane is perpendicular to the centroidal axis of the strand and is the plane where the angle of wire rotation, θ_w is measured. The U-axis is parallel to the X-Y plane and is also parallel to the line on the X-Y plane which specifies the angle of strand rotation. The unit vectors directed along the positive directions of U, V, and W are \mathbf{f} , \mathbf{g} , and \mathbf{h} respectively.

3.3 Vector equations for single and double helices

The model describing the centroidal axis of the central wire of a strand in the rope using the rope co-ordinate system is a single helix model. The model describing the centroidal axis of a wire in a strand using the strand co-ordinate system is also a single helix model. Once these single helix models are formed, they will be used to develop a double helix model describing the centroidal axis of a double helical wire in either a regular lay or a Lang's lay rope in the rope co-ordinate system.

Single helix model

When the rope co-ordinate system is placed at the centre of the wire rope and a certain strand is specified to have an initial strand rotation angle of 0 at $z=0$, as shown in Figure 2A, the vector equation of the helix for the centroidal axis of this strand is:

$$\mathbf{R} = x_s \mathbf{i} + y_s \mathbf{j} + z_s \mathbf{k} \quad (6)$$

The subscript s indicates variables that are associated with a single helix. The parametric equations of \mathbf{R} for a circular strand helix are:

$$x_s = r_s \cos(\theta_s) \quad (7)$$

$$y_s = r_s \sin(\theta_s) \quad (8)$$

$$z_s = r_s \theta_s \tan(\alpha_s) \quad (9)$$

The strand rotation angle, θ_s in Equations 7, 8 and 9 is positive for a right lay rope and negative for a left lay rope.

Similarly, when the strand co-ordinate system is initially placed on the centroidal axis of a certain strand at $\theta_s = 0$, a certain wire is specified to have an initial angle of wire rotation of 0 at $w = 0$, as shown in Figure 2B. The vector equation of the circular helix for the centroidal axis of this wire is similar to Equation 6 in the rope co-ordinate system and can be written as:

$$\mathbf{Q} = u \mathbf{f} + v \mathbf{g} + w \mathbf{h} \quad (10)$$

The parametric equations of \mathbf{Q} for a circular wire helix in a strand are:

$$u = r_w \cos(\theta_w) \quad (11)$$

$$v = r_w \sin(\theta_w) \quad (12)$$

$$w = r_w \theta_w \tan(\alpha_w) \quad (13)$$

The wire rotation angle, θ_w in Equations 11, 12, and 13 is positive if it forms a right-hand strand and is negative if it forms a left-hand strand. Since the co-ordinate system is moving along the centroidal axis of the strand, w simply represents the path length along the centroidal axis that the system has travelled for a wire rotation angle of θ_w .

Double helix model

The double helix model can be developed by properly combining the vector \mathbf{R} in the rope co-ordinate system and a vector \mathbf{q} on the U-V plane of the strand co-ordinate system as shown in Figure 3.

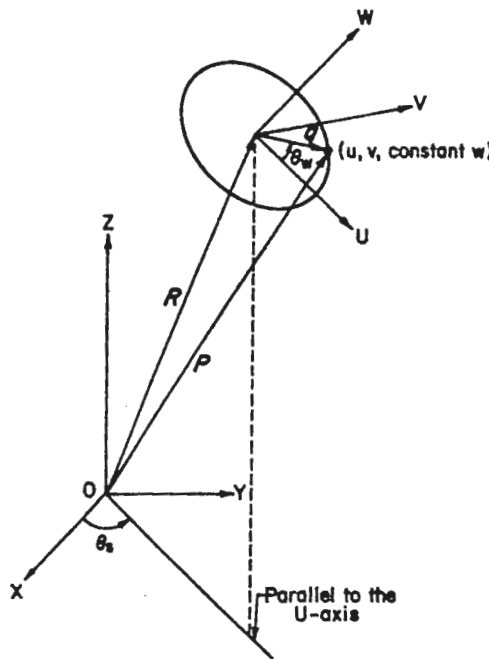


Figure 3: Co-ordinate system for double helix

It is assumed that, in the rope co-ordinate system, a position vector \mathbf{P} with the head of the vector located at (u, v, w) of the strand co-ordinate system traces the centroidal axis of a double helical wire and has a general form:

$$\mathbf{P} = x_w \mathbf{i} + y_w \mathbf{j} + z_w \mathbf{k} \quad (14)$$

where x_w , y_w , and z_w are the component functions. The subscript w indicates variables that are associated a double helix.

The vector \mathbf{q} in the strand co-ordinate system is a position vector which traces the centroidal axis of a double helical wire on the U-V plane at a certain value of w in the strand co-ordinate system. The vector equation for \mathbf{q} may be written as

$$\mathbf{q} = u \mathbf{f} + v \mathbf{g} \quad (15)$$

The w component is not needed in specifying the location of the centroidal axis of a double helical wire because \mathbf{q} is always on the U-V plane. The parametric equations for u and v are identical to Equations 11 and 12.

Since the head of \mathbf{R} is located exactly at the tail of \mathbf{q} , the vector \mathbf{P} can be readily obtained through vector addition once the vector \mathbf{q} in the strand co-ordinate system is

projected to the rope co-ordinate system. Using the fact that the U-axis is parallel to the X-Y plane and the line which specifies the angle of strand rotation (θ_s) and that the U-V plane is perpendicular to the W-axis which has an angle of strand helix (α_s), the individual projections of u and v on the X, Y, and Z axes are:

$$x_u = u \cos(\theta_s) \quad (16)$$

$$y_u = u \sin(\theta_s) \quad (17)$$

$$z_u = 0 \quad (18)$$

$$x_v = -v \sin(\alpha_s) \sin(\theta_s) \quad (19)$$

$$y_v = v \sin(\alpha_s) \cos(\theta_s) \quad (20)$$

$$z_v = -v \cos(\alpha_s) \quad (21)$$

The vector q now can be expressed in the rope co-ordinate system as:

$$q = (x_u + x_v) \mathbf{i} + (y_u + y_v) \mathbf{j} + (z_u + z_v) \mathbf{k} \quad (22)$$

Because the vector P is the sum of R and q , the general form of the vector equation for P now can be written as:

$$P = (x_s + x_u + x_v) \mathbf{i} + (y_s + y_u + y_v) \mathbf{j} + (z_s + z_u + z_v) \mathbf{k} \quad (23)$$

By introducing the relative rotation, n (defined by Equation 5), into Equations 7, 8, 9, 16, 17, 19 and 20, replacing u and v with Equations 11 and 12, and substituting them into equation 23, the following component functions for the double helix model in terms of only wire rotation angle are obtained.

$$x_w = r_s \cos(\theta_w/n) + r_w \cos(\theta_w) \cos(\theta_w/n) - r_w \sin(\alpha_s) \sin(\theta_w) \sin(\theta_w/n) \quad (24)$$

$$y_w = r_s \sin(\theta_w/n) + r_w \cos(\theta_w) \sin(\theta_w/n) + r_w \sin(\alpha_s) \sin(\theta_w) \cos(\theta_w/n) \quad (25)$$

$$z_w = r_s \tan(\alpha_s) \theta_w/n - r_w \cos(\alpha_s) \sin(\theta_w) \quad (26)$$

The sign for θ_w is positive when it rotates anti-clockwise and negative when it rotates clockwise. The lay type determines the sign for n as defined by Equation 5. The component z_w is always positive and increases in the direction that the helix advances.

3.4 Example for a specific wire rope

The circular helix models presented above are applicable to any type of rope construction as long as its strands are round, that is, the wires are laid in a circular pattern. As an example, the structural parameters of a 33-mm 6x19 Seale, IWRC, right regular lay wire rope are used to show how the model for a specific rope is obtained.

The basic strand arrangement of a 6x19 Seale wire rope is shown in Figure 4. The structural parameters of different strands are presented in Table 1. The strand cross sections perpendicular to the strand or wire helix axis are shown in Figures 5 through 7. The structural parameters of the single and double helical wires in each strand are presented in Table 2. Some of the parameters such as the lay length of strand, the lay length of wire, and the relative rotation were calculated based on the basic relationships given by Equations 1, 3, and 5.

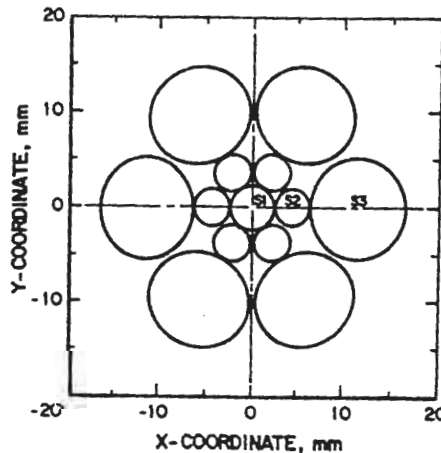


Figure 4: Strand arrangement of 33 mm 6x19 Seale, IWRC, right regular lay wire rope

Strand	Form	No. of strands	Strand radius (mm)	Helix parameters		
				r_s (mm)	a_s (rad)	L_s (mm)
IWRC:						
S1	Straight	1	2.271	NAp	NAp	NAp
S2	Single helix	6	2.016	4.287	1.2362	77.48
Seale:						
S3	Single helix	6	5.110	11.413	1.2259	199.61

NAp Not applicable

Table 1: Structural parameters of strands in 33 mm 6x19 Seale wire rope

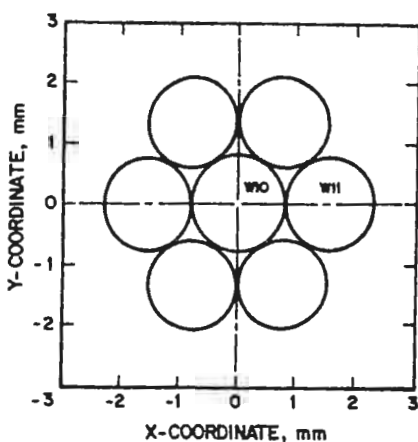


Figure 5: Cross section of IWRC strand S1

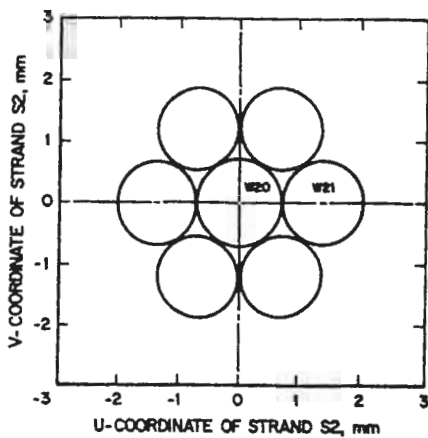


Figure 6: Cross section of IWRC strand S2

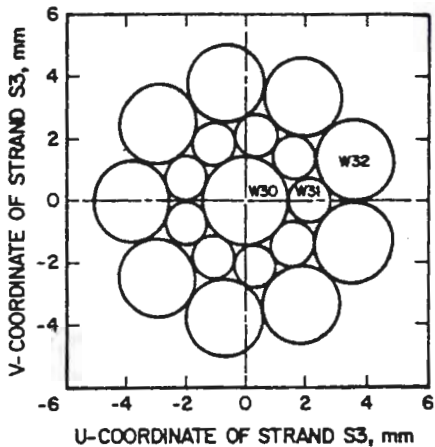


Figure 7: Cross section of Seale strand S3

Wire W21:

$$x_w = 4.287 \cos\left(\frac{\theta_w}{1.5087}\right) + 1.360 \cos(\theta_w) \cos\left(\frac{\theta_w}{1.5087}\right) - 1.285 \sin(\theta_w) \sin\left(\frac{\theta_w}{1.5087}\right) \quad (24a)$$

$$y_w = 4.287 \sin\left(\frac{\theta_w}{1.5087}\right) + 1.360 \cos(\theta_w) \sin\left(\frac{\theta_w}{1.5087}\right) + 1.285 \sin(\theta_w) \cos\left(\frac{\theta_w}{1.5087}\right) \quad (25a)$$

$$z_w = 8.173 \theta_w - 0.447 \sin(\theta_w) \quad (26a)$$

Wire W30:

$$x_s = 11.413 \cos(\theta_s) \quad (7c)$$

$$y_s = 11.413 \sin(\theta_s) \quad (8c)$$

$$z_s = 31.768 \theta_s \quad (9c)$$

Wire W31:

$$x_w = 11.413 \cos\left(\frac{\theta_w}{-3.3855}\right) + 2.168 \cos\left(\frac{\theta_w}{-3.3855}\right) - 2.040 \sin(\theta_w) \sin\left(\frac{\theta_w}{-3.3855}\right) \quad (24b)$$

$$y_w = 11.413 \sin\left(\frac{\theta_w}{-3.3855}\right) + 2.168 \cos(\theta_w) \sin\left(\frac{\theta_w}{-3.3855}\right) + 2.040 \sin(\theta_w) \cos\left(\frac{\theta_w}{-3.3855}\right) \quad (25b)$$

$$z_w = -9.384 \theta_w - 0.733 \sin(\theta_w) \quad (26b)$$

Wire W32:

$$x_w = 11.413 \cos\left(\frac{\theta_w}{-3.3855}\right) + 3.867 \cos(\theta_w) \cos\left(\frac{\theta_w}{-3.3855}\right) - 3.639 \sin(\theta_w) \sin\left(\frac{\theta_w}{-3.3855}\right) \quad (24c)$$

$$y_w = 11.413 \sin\left(\frac{\theta_w}{-3.3855}\right) + 3.867 \cos(\theta_w) \sin\left(\frac{\theta_w}{-3.3855}\right) + 3.639 \sin(\theta_w) \cos\left(\frac{\theta_w}{-3.3855}\right) \quad (25c)$$

$$z_w = -9.384 \theta_w - 1.307 \sin(\theta_w) \quad (26c)$$

4. Model applications

The model for a specific wire rope can be easily obtained, as shown in the example, and has many practical applications. It can be used to generate the wire paths and to evaluate the geometric properties of the wires. The effect of deformation can be determined by substituting the structural parameters of the deformed rope into the original model. The model also has other applications such as predicting damage patterns through external and internal wear, examining and improving the design of a rope construction prior to manufacturing, and producing three-dimensional pictures of the wires for analysis with a computer.

4.1 Generation of wire paths

As described earlier, the wires in wire ropes have three forms: straight, single helix or double helix. The only straight wire in a rope is the centre wire in an independent wire rope core. The wires around the centre wire forming the centre strand and the centre wires in the outer strands of the core and in the surface strands have the shape of a single helix. The wires forming the strand around the centre wire have double-helical paths which are very complex in their configurations. Using the model developed in this report, the wire paths can be easily generated by a computer. They not only will reveal the shapes of the wire paths but also are useful in locating the places where a wire will be rubbed by the other wires and in determining the interval at which an outer wire will be exposed on the rope surface.

Typical paths of single helical wires generated by Equations 7a to 9a, 7b to 9b, and 7c to 9c for wires W11, W20 and W30, respectively, are shown in Figure 8. The paths shown are in about one lay of strand S3. Typical paths of double helical wires generated by Equations 24a to 26a, 24b to 26b and 24c to 26c for wires W21, W31 and W32, respectively, are shown in Figures 9 through 11. The paths shown are in about two lays of the strand formed by each wire. The reason for the major difference between the shape of the W21 path and that of the W31 and W32 paths is because strand S2 which contains wire W21 is a Lang's lay strand while strand S3 which contains W31 and W32 is a regular lay strand. The side views of all wire paths show much sharper turns than the actual wire paths. This is because much larger scales have been selected on the Y co-ordinate than those on the Z co-ordinate of these figures so that more of their paths can be viewed.

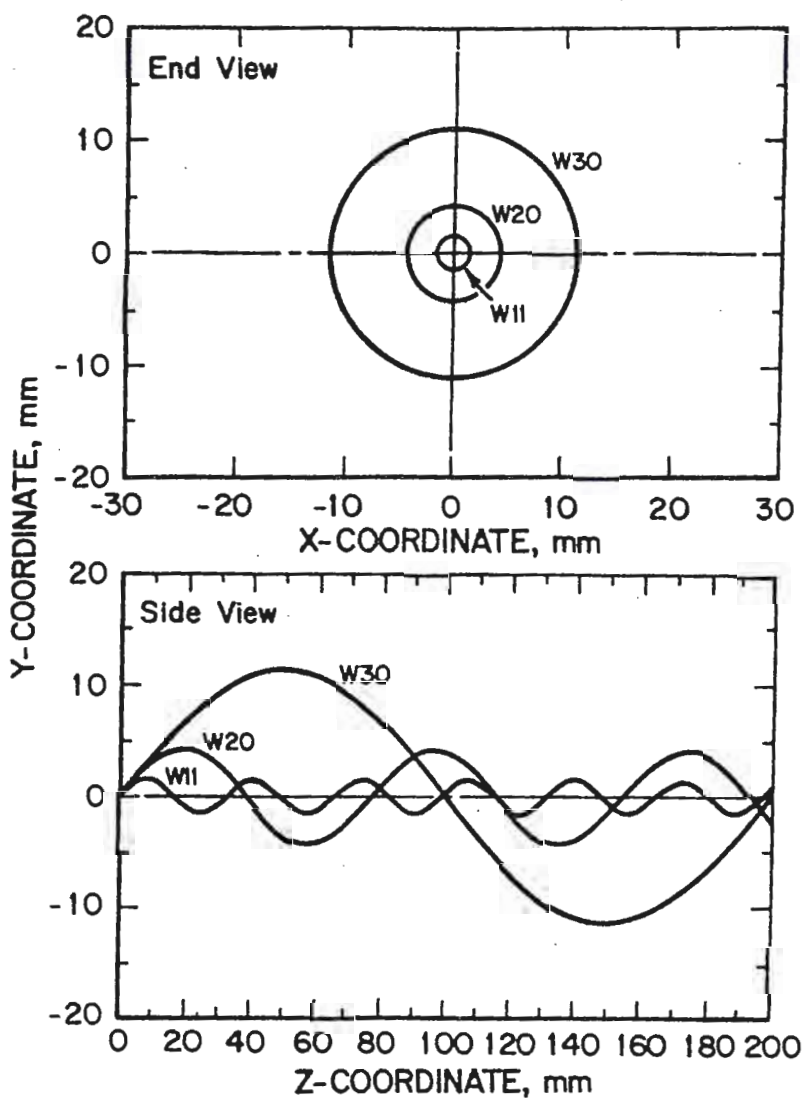


Figure 8: Paths of single helical wires W11, W20, W30

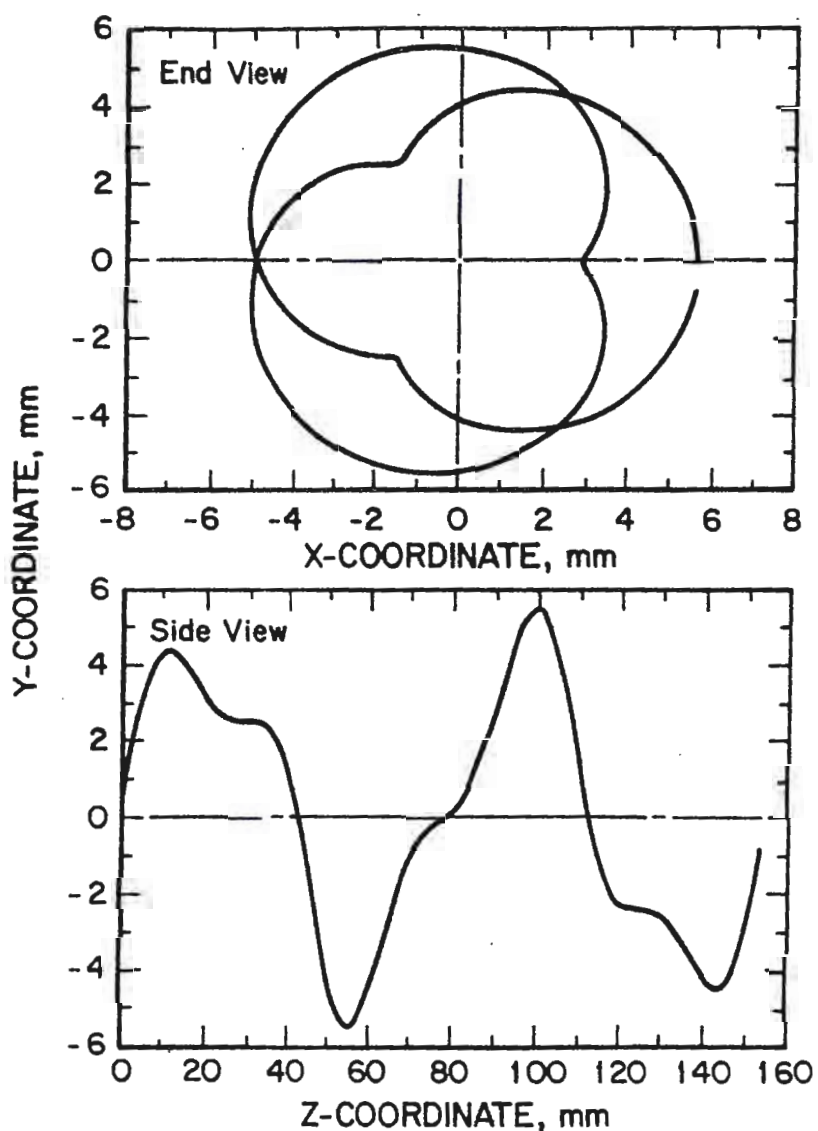


Figure 9: Path of double helical wire W21

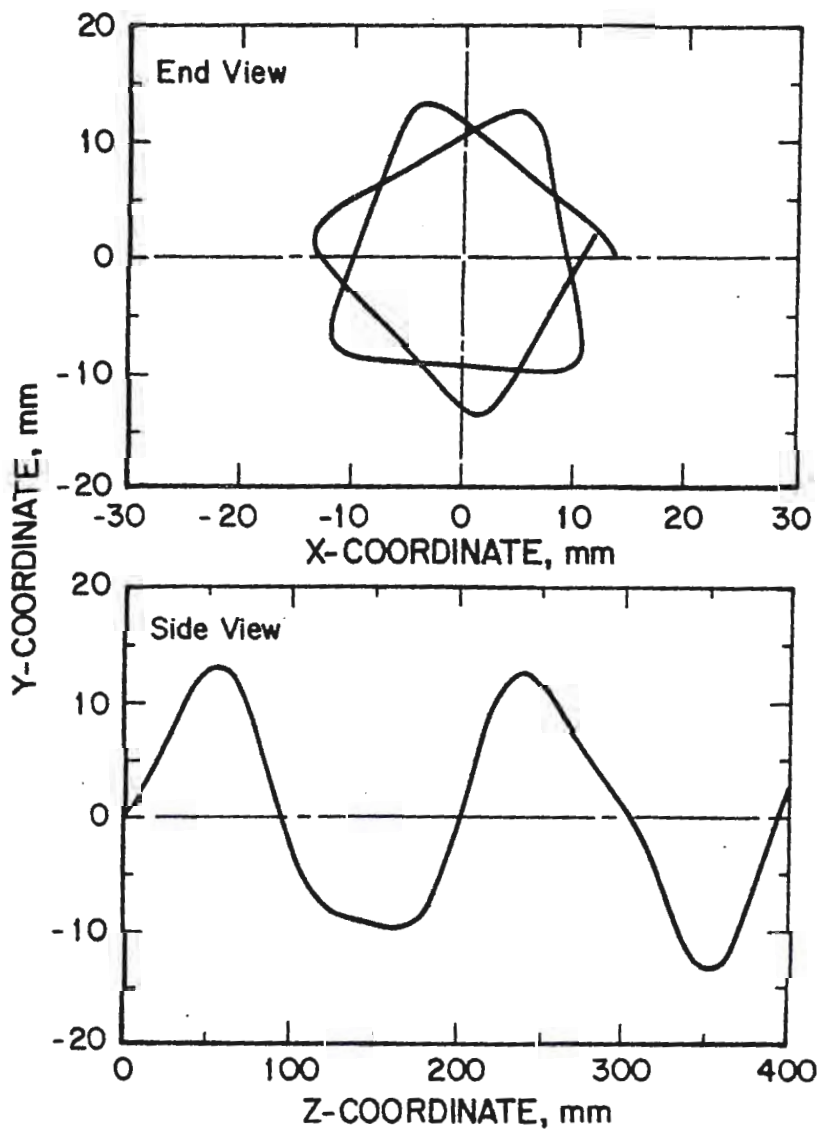


Figure 10: Path of double helical wire W31

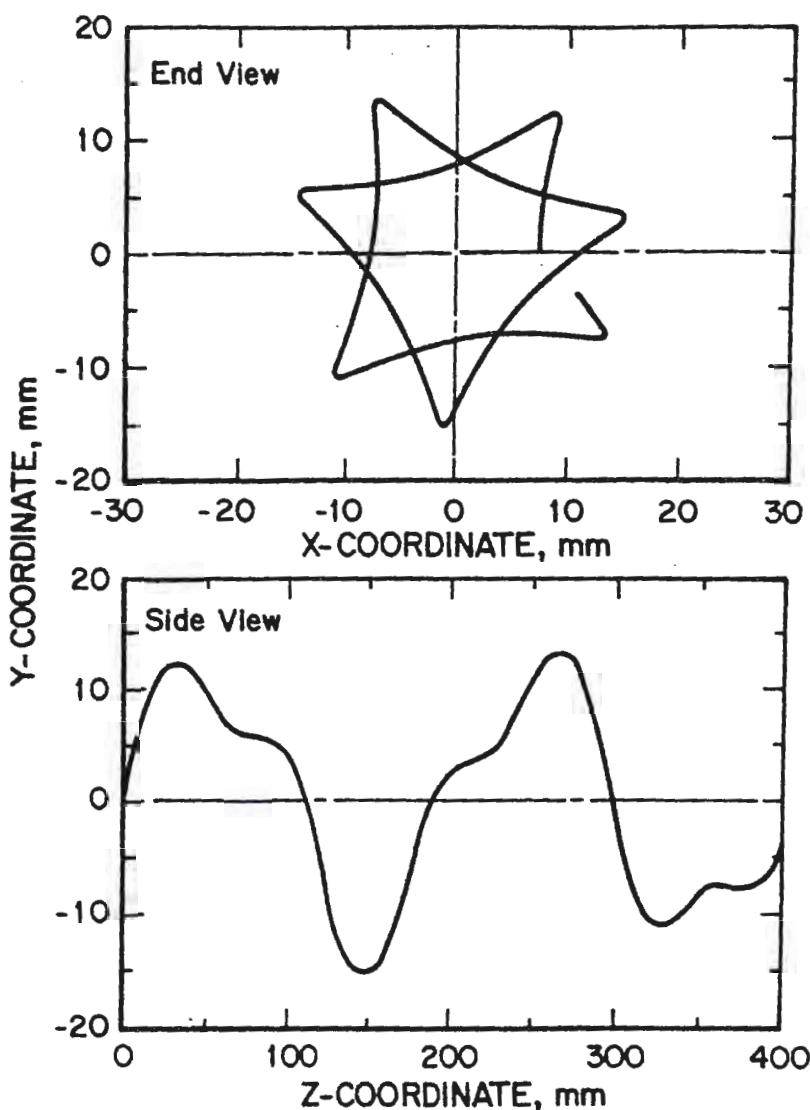


Figure 11: Path of double helical wire W32

4.2 Evaluation of geometric properties

In order to know how the tensile load is distributed among the wires in a rope and to calculate wire stresses, several geometric properties of each wire must be evaluated before and after the application of load. These properties are the path length, the curvature and the torsion.

Path length per lay of strand

The equations for evaluation of the path length of single and double helical wires in each lay of the strand can be derived from Equations 2 through 4 and are shown in Equations 27 and 28.

Path length of single helical wires in each lay of strand:

$$S_s = \frac{2\pi r_s}{\cos(\alpha_s)} \quad (27)$$

Path length of double helical wires in each lay of strand:

$$S_w = \frac{2\pi r_s}{\cos(\alpha_s) \sin(\alpha_w)} \quad (28)$$

Table 3 shows the path lengths per lay of strand for a 6x19 Seale rope as calculated by these two equations. The table also shows the wire-to-rope length ratios by comparing the wire paths to the strand lay lengths.

Wire	Lay length of strand referred to	Lay length of strand L_s (mm)	Path length per lay of strand (mm)	Wire-to-rope length ratio
Straight:				
W10	NAp	NAp	NAp	1.000
Single helical:				
W11	L_{11}	33.02	34.40	1.042
W20	L_{20}	77.48	82.03	1.059
W30	L_{30}	199.61	212.10	1.063
Double helical:				
W21	L_{20}	77.48	83.04	1.072
W31	L_{30}	199.61	217.06	1.087
W32	L_{30}	199.61	227.50	1.140

NAp Not applicable

Table 3: Path length of wires per lay of strand

Curvature

A special moving frame of reference has been used in generation of the basic equations for evaluation of the curvature and torsion of a curve in three-dimensional space (Sokolnikoff & Redheffer, 1958 and Leithold, 1986). This frame is formed by a three-dimensional, right-handed set of orthogonal unit vectors as shown in Figure 12. The origin of the frame is located at the head of any position vector that may be R or P of the models just developed. The three unit vectors t , n , and b are called the unit tangent, the unit principal normal, and the unit bi-normal vectors respectively. The frame is sometimes referred to as the moving tri-hedral associated with the curve.

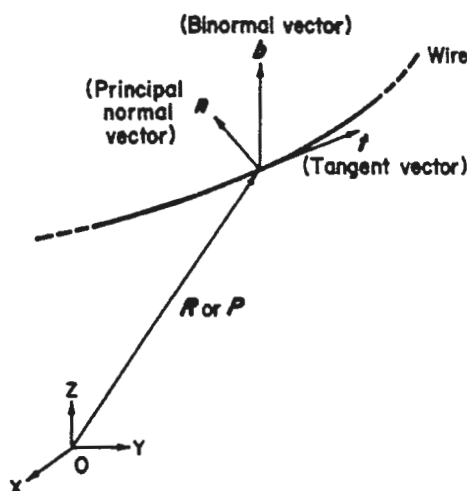


Figure 12: The moving tri-hedral

The curvature at a certain point of a curve is a measure of how quickly the curve changes direction at that point. It is the reciprocal of the radius of the curve at that point and expressed in the unit of 1/mm in this report. In a wire, a change of the curvature is produced by bending moments that act on the wire cross section. Curvature not only is related to the shearing stress but also has effect on the distribution of the tensile stress on the cross section. Therefore, the deformation of the rope structure in terms of the curvature change needs to be specified in order to determine its effect on shearing and normal stresses.

The curvature vector is defined to be the first derivative of t in the moving tri-hedral, as shown in Figure 12, with respect to arc length of a curve. It can be expressed as κn , where κ is a scalar multiplier. The curvature vector is in the same direction of the principal normal vector. The magnitude of this vector is called the curvature of the curve and is simply equal to κ because the magnitude of n is unity. The curvature of a straight line is always zero because the tangent vector is constant. The curvature of the centroidal axis of either a single or a double helical wire, therefore, may be specifically defined to be the magnitude of the rate of change of the unit tangent vector with respect to arc length of the wire.

Basic formulae derived for evaluation of curvature are expressed in terms of the position vector with arc length as the parameter, because arc length arises naturally

from the shape of the curve (Sokolnikoff & Redheffer, 1958). To directly apply the model developed in this paper, it is more convenient to use Equations 29 and 30 for computation of the curvature (Stewart, 1991). The vectors \mathbf{R} and \mathbf{P} denoted with single and double primes in the equations represent the first and second derivatives respectively with respect to θ_s or θ_w , just as for real-valued functions. Similarly, the vectors denoted with triple primes to be used later, represent the third derivatives with respect to θ_s or θ_w . The symbol " $|\cdot|$ ", by which the vector is bounded, represents the magnitude of the vector as is generally used in vector analysis. \mathbf{R} was given by Equation 6 and its component functions were given in Equations 7, 8 and 9. \mathbf{P} was given by Equation 14 and its component functions were given in Equations 24, 25 and 26.

Curvature of single helical wires:

$$\kappa_s = \frac{|\mathbf{R}' \times \mathbf{R}''|}{\mathbf{R}''^3} \quad (29)$$

Curvature of double helical wires:

$$\kappa_w = \frac{|\mathbf{P}' \times \mathbf{P}''|}{\mathbf{P}''^3} \quad (30)$$

Substituting the first and second derivatives of each vector into Equations 29 and 30 and performing the cross and dot product and other operations, the expanded forms of these equations expressed in terms of the component functions are shown below.

Expanded curvature equation for single helical wires:

$$\kappa_s = \frac{\sqrt{(y'_s z''_s - z'_s y''_s)^2 + (z'_s x''_s - x'_s z''_s)^2 + (x'_s y''_s - y'_s x''_s)^2}}{\sqrt{(x'_s)^2 + (y'_s)^2 + (z'_s)^2}^3} \quad (29a)$$

After substituting the functions into Equation 29a, it can be reduced to its simplest form as shown in Equation 29b. This expression indicates that the curvature of a single helical wire is independent of the angle of strand rotation and is constant for a given helix angle.

$$\kappa_s = \frac{\cos^2(\alpha_s)}{r_s} \quad (29b)$$

Expanded curvature equation for double helical wires:

$$\kappa_w = \frac{\sqrt{(y'_w z''_w - z'_w y''_w)^2 + (z'_w x''_w - x'_w z''_w)^2 + (x'_w y''_w - y'_w x''_w)^2}}{\sqrt{(x'_w)^2 + (y'_w)^2 + (z'_w)^2}^3} \quad (30a)$$

The curvatures were computed for both single and double helical wires in a 6x19 Seale wire rope. The results for single helical wires are shown in Table 4. The results for double helical wires are shown in Table 5 with the absolute value of θ_w increasing from 0 to 360 degrees at increments of 15 degrees.

Wire	Curvature (1/mm)	Torsion (1/mm)
W11	0.0513	0.1753
W20	0.0252	0.0724
W30	0.0100	0.0179

Table 4: Curvature and torsion of single helical wires

Angle of wire rotation (°)	Curvature (1/mm)			Torsion (1/mm)		
	W21	W31	W32	W21	W31	W32
0	0.0652	0.0202	0.0265	0.1249	-0.0198	-0.0268
15	0.0649	0.0201	0.0264	0.1256	-0.0200	-0.0273
30	0.0638	0.0197	0.0260	0.1277	-0.0207	-0.0288
45	0.0620	0.0190	0.0254	0.1313	-0.0218	-0.0314
60	0.0593	0.0180	0.0244	0.1365	-0.0233	-0.0353
75	0.0559	0.0167	0.0232	0.1435	-0.0254	-0.0407
90	0.0517	0.0151	0.0216	0.1528	-0.0281	-0.0479
105	0.0467	0.0132	0.0197	0.1653	-0.0319	-0.0580
120	0.0411	0.0110	0.0175	0.1829	-0.0377	-0.0723
135	0.0353	0.0086	0.0152	0.0286	-0.0485	-0.0933
150	0.0297	0.0060	0.0130	0.2460	-0.0757	-0.1234
165	0.0254	0.0033	0.0113	0.2914	-0.1897	-0.1586
180	0.0238	0.0016	0.0106	0.3157	-0.7359	-0.1768
195	0.0254	0.0033	0.0113	0.2914	-0.1897	-0.1586
210	0.0297	0.0060	0.0130	0.2460	-0.0757	-0.1234
225	0.0353	0.0086	0.0152	0.2086	-0.0485	-0.0933
240	0.0411	0.0110	0.0175	0.1829	-0.0377	-0.0723
255	0.0467	0.0132	0.0197	0.1653	-0.0319	-0.0580
270	0.0517	0.0151	0.0216	0.1528	-0.0281	-0.0479
285	0.0559	0.0167	0.0232	0.1435	-0.0254	-0.0407
300	0.0593	0.0180	0.0244	0.1365	-0.0233	-0.0353
315	0.0620	0.0190	0.0254	0.1313	-0.0218	-0.0314
330	0.0638	0.0197	0.0260	0.1277	-0.0207	-0.0288
345	0.0649	0.0201	0.0264	0.1256	-0.0200	-0.0273
360	0.0652	0.0202	0.0265	0.1249	-0.0198	-0.0268

Table 5: Curvature and torsion of double helical wires

The curvatures of the IWRC and S3 helical wires were plotted against the absolute value of the angle of strand or wire rotation. Their relationships are shown in Figure 13 for two periods. They indicate that:

- the curvature of single helical wires is independent of the angle of strand rotation as expressed by Equation 29b;
- the curvature of double helical wires is a periodical function of the angle of wire rotation with a period of 360 degrees; and,
- the curvature of double helical wires is at maximum when the wires are farthermost from the rope centre and is at minimum when the wires are nearest to the rope centre because the angle of wire rotation is measured from the positive U axis which points away from the rope centre as shown in Figure 3.

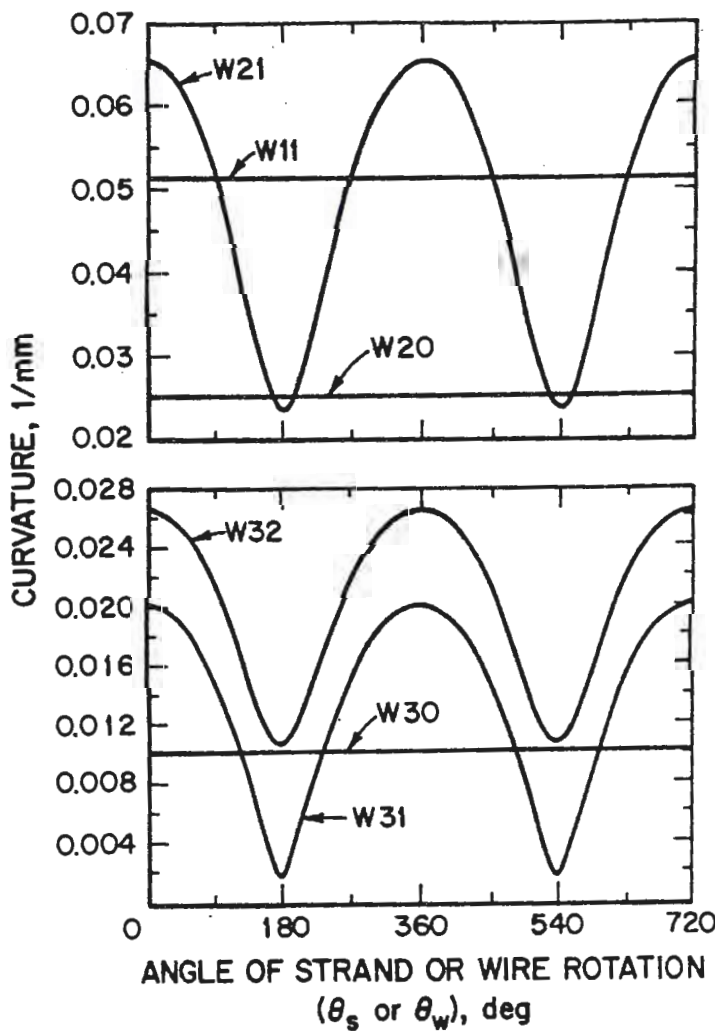


Figure 13: Curvature of IWRC and S3 wires

Torsion

The torsion at a certain point of a curve measures the degree of twisting of a curve at that point. The change of torsion in a wire is produced by twisting moments that act on the wire cross section. Angular deformation between cross sections results in shearing stresses.

The first derivative of \mathbf{b} in the moving tri-hedral, as shown in Figure 12, with respect to arc length of a curve will yield a vector which is parallel to \mathbf{n} and can be expressed as $-\tau\mathbf{n}$. The scalar multiplier τ is called the torsion of the curve. It measures the rate at which the centroidal axis of either a single or a double helical wire twists out of its osculating plane, which is the plane containing the unit tangent and the unit principal normal vectors. The torsion of a straight line is defined to be zero. If the curve is a plane curve, the torsion is always zero because the osculating plane is the plane of the curve and the unit bi-normal vector is constant.

Basic formulae derived for computation of torsion are expressed in terms of the position vector with arc length as the parameter (Sokolnikoff & Redheffer, 1958). To directly apply the models developed in this paper, it is more convenient to use Equations 31 and 32 for computation of the torsion (Stewart, 1991).

Torsion of single helical wires:

$$\tau_s = \frac{\mathbf{R}' \times \mathbf{R}'' \cdot \mathbf{R}''}{|\mathbf{R}' \times \mathbf{R}''|^2} \quad (31)$$

Torsion of double helical wires:

$$\tau_w = \frac{\mathbf{P}' \times \mathbf{P}'' \cdot \mathbf{P}''}{|\mathbf{P}' \times \mathbf{P}''|^2} \quad (32)$$

Substituting the derivatives of each vector into the equations and performing the cross and dot product and other operations, the expanded forms of these equations expressed in terms of the component functions are shown below.

Expanded torsion equation for single helical wires:

$$\tau_s = \frac{x''_s(y'_s z''_s - z'_s y''_s) + y''_s(z'_s x''_s - x'_s z''_s) + z''_s(x'_s y''_s - y'_s x''_s)}{(y'_s z''_s - z'_s y''_s)^2 + (z'_s x''_s - x'_s z''_s)^2 + (x'_s y''_s - y'_s x''_s)^2} \quad (31a)$$

After substituting the functions into Equation 31a, it can be reduced to its simplest form as shown in Equation 31b. It indicates that the torsion of a single helical wire is independent of the angle of strand rotation and is constant for a given helix angle.

$$\tau_s = \frac{\sin(\alpha_s) \cos(\alpha_s)}{r_s} \quad (31b)$$

Expanded torsion equation for double helical wires:

$$\tau_w = \frac{x''_w(y'_w z''_w - z'_w y''_w) + y''_w(z'_w x''_w - x'_w z''_w) + z''_w(x'_w y''_w - y'_w x''_w)}{(y'_w z''_w - z'_w y''_w)^2 + (z'_w x''_w - x'_w z''_w)^2 + (x'_w y''_w - y'_w x''_w)^2} \quad (32a)$$

The torsions of both single and double helical wires in a 6x19 Seale wire rope were computed. The results for single helical wires are shown in Table 4. The results for double helical wires are shown in Table 5 with the absolute value of θ_w increasing from 0 to 360 degrees at increments of 15 degrees. The negative torsions for W31 and W32 represent the twisting of the centroidal axes of these wires in a left lay strand, where the twisting is opposite in direction to that in a right lay strand.

The torsions of the IWRC and S3 helical wires were plotted against the absolute value of the angle of wire rotation. Their relationships are shown in Figure 14 for two periods. They indicate that:

- the torsion of single helical wires is independent of the angle of strand rotation as expressed by Equation 31b;
- the torsion of double helical wires is a periodical function of the angle of wire rotation with a period of 360 degrees; and,
- the torsion of double helical wires is at minimum when the wires are farthest from the rope centre and is at maximum when the wires are nearest to the rope centre.

It is also noted that the minimum torsion occurs at the locations where the curvature is at maximum and the maximum torsion occurs at the locations where the curvature is at minimum.

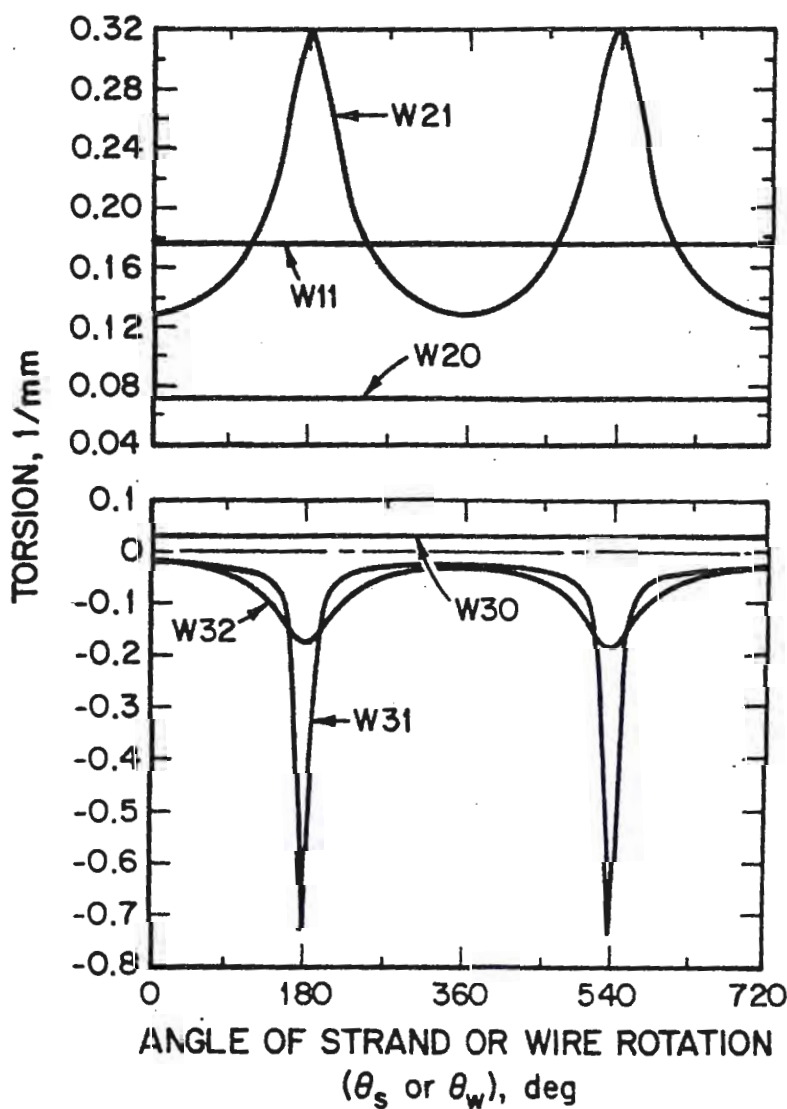


Figure 14: Torsion of IWRC and S3 wires

4.3 Model for the deformed rope

When a tensile load is applied to a wire rope, each individual wire will deform. Because of the differences in the wire lengths and the helix angles of single and double helical wires, the load will not be distributed among the wires simply based on the cross-sectional areas. The effect of these wire deformations on the geometry of the rope structure needs to be determined. The major change is axial elongation along the centroidal axis of a wire. Accompanying the axial elongation is a lateral contraction of the cross section. In addition, bending and twisting moments are generated in the wire that cause the changes in the curvature and torsion of the wire. The combination of all of these individual wire deformations result in the deformation of the rope structure.

There will be a resultant twisting moment which will cause the rope to rotate if the ends are not restrained. Therefore, the deformation of the rope structure will depend on whether the rope is allowed to rotate or not. In mine hoisting, the cage or skip and rope are prevented from rotating by the shaft guides. Some rope manufacturers also produce rotation-resistant rope (Wire Rope Technical Board, 1993), which is made with layers of strands laid in opposite directions to produce counteracting torques. In the use of rope with both ends restrained, the total number of strand lays and the total number of wire lays in a rope are kept constant. Thus, the relative rotation, n , included in the models for double helical wires, remains constant as the rope structure deforms under load. A system of equations can be established for determining the structural parameters of the deformed rope at a given rope strain, thus obtaining the model for the deformed rope. The geometric properties of each deformed wire can be evaluated the same way as shown in this report for the undeformed rope.

5. Conclusions

The model developed in this report fully describes the geometry of the structure of wire ropes of any round-strand construction. It is expressed by vector equations in a three-dimensional, right-handed rectangular Cartesian co-ordinate system and is general enough that any combination of wire and strand lay directions can be handled, being careful only to observe the stated sign conventions for the angles of strand and wire rotation and the relative rotation in the component functions.

The wire paths are defined for the first time by using a developed model, which not only reveal the shapes of the various wires but also are useful for predicting damage patterns through external and internal wear. The geometric properties of each wire can be easily evaluated by using this model. An analysis for a 33-mm 6x19 Seale IWRC, right regular lay wire rope was made to illustrate the usefulness of the model.

6. References

CFR (1997) *Code of Federal Regulations*. Washington, DC: U.S. Government Printing Office, Office of the Federal Register, 30 CFR 56.19024, 57.19024, 75.1434, 77.1434.

Costello, G.A. (1990) *Theory of wire rope*. New York, NY: Springer-Verlag, pp. 53-54.

Leithold, L. (1986) *The calculus with analytic geometry*. 5th ed. New York, NY: Harper & Row, Publisher, Inc., pp. 1072-1077.

Lee, W.K. (1991) *An insight into wire rope geometry*. Int J Solids Structures 28:4:471-490.

Sokolnikoff, I.S. & Redheffer, R.M. (1958) *Mathematics of physics and modern engineering*. New York, NY: McGraw-Hill Book Co., Inc., pp. 311-315.

Stewart, J (1991) *Calculus*. 2nd ed. Pacific Grove, CA: Brooks/Cole Publishing Co., pp. 688-691.

Wire Rope Technical Board (1993) *Wire Rope Users Manual*. 3rd ed. Woodstock, MD: Wire Rope Technical Board.